

# <sup>1</sup> Brief communication: Intercomparison study reveals pathways for <sup>2</sup> improving the representation of sea-ice biogeochemistry in models

<sup>3</sup> Letizia Tedesco<sup>1</sup>, Giulia Castellani<sup>2</sup>, Pedro Duarte<sup>3</sup>, Meibing Jin<sup>4</sup>, Sebastien Moreau<sup>3</sup>, Eric Mortenson<sup>5</sup>,  
<sup>4</sup> Benjamin Tobey Saenz<sup>6</sup>, Nadja Steiner<sup>7,8,9</sup>, Martin Vancoppenolle<sup>10</sup>

<sup>5</sup> <sup>1</sup>Marine and Freshwater Solutions, Finnish Environment Institute, Helsinki, Finland

<sup>6</sup> <sup>2</sup>Institute of Environmental Physics (IUP), MARUM – Center for Marine Environmental Sciences, University of Bremen,  
7 Bremen, Germany

<sup>8</sup> <sup>3</sup>Norwegian Polar Institute, Tromsø, Norway

<sup>9</sup> <sup>4</sup>University of Alaska Fairbanks, AK, USA

<sup>10</sup> <sup>5</sup>University of Miami, Cooperative Institute for Marine and Atmospheric Studies (CIMAS)

<sup>11</sup> <sup>6</sup>Biota.Earth, Berkeley, CA, USA

<sup>12</sup> <sup>7</sup>Institute of Ocean Sciences, Fisheries and Oceans Canada, Sidney, BC, Canada

<sup>13</sup> <sup>8</sup>Canadian Center for Climate Modelling and Analysis, Environment and Climate Change Canada, Victoria, BC, Canada

<sup>14</sup> <sup>9</sup>School of Earth and Ocean Sciences, University of Victoria, Victoria, BC, Canada

<sup>15</sup> <sup>10</sup>Laboratoire d'Océanographie et du Climat, CNRS/IRD/MNHN, Sorbonne Université, Paris, France

<sup>16</sup>

<sup>17</sup> Correspondence to: Letizia Tedesco (letizia.tedesco@environment.fi)

<sup>18</sup>

<sup>19</sup> **Abstract.** Sea-ice biogeochemical models are key to understanding polar marine ecosystems. We present an intercomparison  
<sup>20</sup> of six one-dimensional sea-ice biogeochemical models, assessing their ability to simulate algal phenology and nutrient  
<sup>21</sup> dynamics by comparing them with sea-ice physical-biogeochemical data collected during an Arctic drift expedition in spring  
<sup>22</sup> 2015. While no model fully captured observed bloom dynamics using their default parameter set, tuning improved biomass  
<sup>23</sup> simulations but had a limited impact on nutrient representation. Variability in tuning strategies underscores key knowledge  
<sup>24</sup> gaps and the need for further model development in more harmonised ways. Our findings can inform future efforts to  
<sup>25</sup> enhance the reliability and predictive capacity of sea-ice biogeochemical models.

## <sup>26</sup> 1 Introduction

<sup>27</sup> Sea ice is home to an active microbial community, with ice algae displaying some of the highest Chlorophyll-a (Chl-a)  
<sup>28</sup> concentrations of any aquatic environment (Arrigo, 2017). Ice algae play multiple pivotal roles in polar oceans, representing  
<sup>29</sup> the largest biomass fraction in sea ice (Poulin et al., 2011), contributing to overall marine primary production (Dalman et al.,  
<sup>30</sup> 2025), acting as a critical food source for the marine food web, especially during winter (Schaafsma et al., 2017), and  
<sup>31</sup> efficiently contributing to the ocean carbon sink (Boetius et al., 2013). Together with phytoplankton, ice algae form the  
<sup>32</sup> foundation of the polar marine food web, supporting key under-ice foraging species such as Arctic cod (*Boreogadus saida*)  
<sup>33</sup> in the Arctic Ocean (Geoffroy et al., 2023) and Antarctic krill (*Euphausia superba*) in the Southern Ocean (Kohlbach et al.,

34 2017). These species depend on the presence of sea ice and play a crucial role in transferring carbon to higher trophic levels,  
35 including humans (Steiner et al., 2021).

36

37 Current environmental changes are placing considerable pressure at the base of the food web, triggering significant effects  
38 throughout trophic levels (e.g., Post et al., 2013; Koch et al., 2023). Despite the recognised importance of the sea-ice  
39 ecosystems (Lannuzel et al., 2020), our knowledge remains limited due to their remote location and extreme weather  
40 conditions, which restrict observational data - particularly biological observations - to sparse spatial and temporal  
41 distributions. As a result, the representation of sea-ice biological and ecological processes in numerical models has  
42 historically been limited. However, in recent decades, significant advances have been made in modelling sea-ice habitats and  
43 the evolution of sea-ice biological communities (Castellani et al., 2025). Progress includes improved representation of  
44 physical processes, greater biodiversity, and enhanced ecosystem complexity.

45

46 An intercomparison of three-dimensional models has already been conducted to understand similarities and differences in  
47 simulated ice algae abundance and distribution, the Ice Algae Model Intercomparison Project – Phase 1 (IAMIP1, Watanabe  
48 et al., 2019). This study investigated the seasonal-to-decadal variability in ice-algal primary productivity across four Arctic  
49 regions during 1980–2009, as simulated by five participating models. Its conclusions indicated that, despite the ongoing  
50 reduction in Arctic sea ice, the decadal trend in ice-algal productivity remained unclear. The vernal bloom shifted towards an  
51 earlier onset and shorter duration over the simulated period, and the choice of maximum algal growth rate was identified as a  
52 key driver of inter-model differences in simulated ice-algal primary productivity. A second phase, expanding the study's  
53 scope to global coverage and centennial timescales following CMIP6 (Coupled Model Intercomparison Project Phase 6,  
54 Eyring et al., 2016) protocols, is currently underway (IAMIP2, Hayashida et al., 2021). However, given the numerous  
55 limitations and uncertainties associated with these large-scale models, they are more useful for deriving bulk properties than  
56 for investigating more detailed ecological processes.

57

58 To this end, one-dimensional (1D) process models become essential for addressing knowledge gaps in sea-ice  
59 biogeochemistry and ecological dynamics, as they provide a level of detail that large-scale models lack. They also allow for  
60 direct comparisons with in-situ observations, improving the ability to validate results. However, existing process models  
61 have been developed independently during periods of limited observations and incomplete process understanding, validated  
62 by observations at different locations, leading to substantial differences across models. These differences make an  
63 intercomparison of models performances challenging. To address this, the BEPSII (Biogeochemical Exchange Processes at  
64 Sea-Ice Interfaces, <https://www.bepsii.org>) expert group initiated an intercomparison of 1D sea-ice biogeochemical models,  
65 presented here, aiming at: i) understanding variability among models in representing key processes and responses to a  
66 common set of boundary conditions, ii) identifying divergences in models' behaviour, the variety of tuning strategy, and the  
67 drivers of model sensitivity, iii) testing transferability, and finally iv) promoting harmonisation for future model

68 developments. The focus has been on understanding the similarities and differences in simulated ice algal dynamics and  
69 investigating the controlling factors responsible for the temporal variability and magnitude of ice-algal productivity among  
70 participating 1D models.

71

72 We present in this study an intercomparison of 1D sea-ice biogeochemical models (briefly described in Sect. 2.1 and more  
73 comprehensively in the Supplementary Material), focusing on their ability to simulate ice algal dynamics and nutrient  
74 cycling. Using a refrozen lead time series (described in Sect 2.2) as a test case, we assess model performance through a  
75 structured comparison of simulated and observed biogeochemical variables. Two experiments - *no tuning* and *tuning* - were  
76 conducted (Sect 2.3) to evaluate the baseline model configurations as well as the impact of targeted parameter adjustments  
77 on model accuracy. We analyse differences in model outputs, identify key sources of variability, and discuss the challenges  
78 associated with simulating ice algal growth and nutrient fluxes (Sect 3). Finally, we highlight the implications of our findings  
79 for future model development and propose directions for improving the representation of biogeochemical processes in  
80 sea-ice models (Sect. 4).

## 81 2 Methods

### 82 2.1 Sea-ice biogeochemical models

83 1D process models are typically designed to represent only vertical processes, assuming that horizontal advection is  
84 negligible. Since they are computationally efficient, these models can incorporate a high level of ecosystem complexity, such  
85 as representing multiple functional groups of organisms and providing high vertical resolution by discretising sea ice into  
86 several layers.

87

88 1D sea-ice biogeochemical models vary in vertical resolution, ecosystem complexity, and whether they are coupled to the  
89 ocean and/or atmosphere (Castellani et al., 2025). The biogeochemically active part of sea ice, also known as the  
90 Biologically Active Layer (BAL) (Tedesco et al., 2010), is represented either as a single layer near the ice-ocean interface of  
91 prescribed or variable thicknesses depending on sea-ice permeability, or as multiple layers spanning the vertical range of the  
92 sea ice with an active brine network (e.g., Jeffery et al., 2016). Single-layer approaches are computationally more efficient  
93 than multi-layer models. A single-layer model of variable thicknesses in response to thermodynamic growth, often referred  
94 to as dynamic layering, provides a more realistic representation of bottom community dynamics (Tedesco et al., 2010).  
95 Multi-layer models, on the other hand, capture the vertical variability of biogeochemical variables and allow simulating  
96 surface and infiltration communities.

97

98 As in ocean models, the structure of sea-ice microbial ecosystems is represented using a set of “Plankton Functional Types”  
99 (PFTs, e.g., sea-ice algae and bacteria) and non-living inorganic (e.g., sea-ice micro- and macronutrients) and organic matter

100 (e.g., sea-ice detritus). The simplest models are N-P models, which include only one nutrient (N) and one algal functional  
101 type (P). The elemental composition of ice algae is typically fixed, based on prescribed Redfield carbon, nitrogen, silicon,  
102 phosphorous ratios (106:16:16:1), along with fixed Chl-a:carbon ratios. The more comprehensive N-P-Z-D models also  
103 include grazers (Z) (such as sea-ice fauna) and sea-ice detritus (D). In the simplest version of these models, only one limiting  
104 nutrient is considered. More complex models may represent multiple nutrients and different PFTs for ice algal communities,  
105 as well as bacteria and grazers. In simpler models, the processes associated with bacterial remineralisation or grazing are  
106 often implicitly parameterised using constant rates.

107

108 The intercomparison included five modelling teams and a total of six model configurations. These models varied in several  
109 aspects, encompassing differences in physical (from Semtner 0-layer to energy-conserving multi-layer models) and  
110 biogeochemical process complexity (from a single PFT to several PFTs), radiation schemes (from a single band  
111 Lambert-Beer to a multi-band Delta-Eddington), vertical resolution (from a static single layer to dynamic multi layers),  
112 choice of limiting nutrient (from one single nutrient limiting to multi-nutrient limitation), area of original tuning of the  
113 model, and coupling to an interactive sea-ice physical model and/or ocean biogeochemical model of various complexity  
114 (from none to fully resolved). Table 1 summarises the main commonalities and differences among the models. For more  
115 details on a specific model, we refer to the model's original reference (Table 1) and further description in the Supplementary  
116 Material.

117

118 Most of the models had interactive physical components, while only one (i.e., SIMBA) required prescribed ice physics.  
119 Additionally, only half of the models were coupled to an interactive ocean biogeochemical model. Among the sea-ice  
120 physical models, complexities ranged from a Semtner 0-layer scheme (SM 0L) to multi-layer energy-conserving models  
121 (EC ML). All models, except one, used a single-band radiation transfer scheme, with several assuming Beer-Lambert (BL)  
122 light attenuation, while only one employed a Delta-Eddington (DE) scheme. The majority of the models simulated ice algae  
123 only in the bottom sea-ice layer, either as a static or dynamic system, while two models were multi-layer models, simulating  
124 ice algae along the entire ice column. In terms of ecosystem complexity, models varied from simple Redfield-based models  
125 (RFD) with a single limiting nutrient, one algal group, and a detritus compartment to more comprehensive quota models with  
126 several functional groups, including ice bacteria, ice fauna, and multi-nutrient limitations.

## 127 2.2 The N-ICE2015 Dataset

128 The refrozen lead time series monitored during the N-ICE2015 expedition (Granskog et al., 2018) was selected as a test case  
129 for the model intercomparison due to the high frequency of available physical and biogeochemical measurements (e.g.  
130 Kauko et al., 2017; Olsen et al., 2017). The N-ICE expedition was a field campaign conducted aboard the RV *Lance*, which  
131 was frozen into pack ice north of Svalbard, drifting between approximately 83° and 80°N in the southern Nansen Basin of  
132 the Arctic Ocean between January and June 2015. Among the four ice floes monitored during the study period, the refrozen

133 lead data were derived from Floe 3, which was studied from mid-April to early June 2015 as it drifted southward from 81.8°  
134 N to 80.5° N.

135

136 **Table 1:** Sea-ice biogeochemical models participating in the 1D intercomparison project. BGC stands for biogeochemistry. Please see the  
137 main text for the remaining nomenclature used in the table.

Model/ Properties	BFM-SI	BFM-SI-Clim	CICE 5.1	CSIB-1D	SIESTA	SIMBA
<b>Ice Physics</b>	Modified SM 0L	Modified SM 0L	EC ML	SM 0L	EC ML	Prescribed
<b>Transport</b>	Growth/melt	Growth/melt	Growth/melt, brine drainage/diffus ion	Melt	Desalination	Growth/melt
<b>Radiation</b>	1 band; BL	1 band; BL	1 band; BL	1 band; BL	32 bands; DE	1 band; BL
<b>Grid for sea ice BGC</b>	1L, bottom, dynamic	1L, bottom, dynamic	Multi-layer	1L bottom static	Multi-layer	1L bottom static
<b>Sea-ice functional groups</b>	3N-2P-2D-1B-1Z	3N-1P-2D	2N-1P	2N-1P-1D	3N-1P-1D	1N-1P-1D
<b>Cell quotas/Chl:C</b>	Quota/Prognostic	Quota/Prognostic	RFD/Constant	RFD/Constant	RFD/Constant	RFD/Constant
<b>Limiting element(s)</b>	Nitrogen, Phosphorous, Silicon	Silicon	Nitrogen, Silicon	Nitrogen, Silicon	Nitrogen, Phosphorous, Silicon	Nitrogen
<b>Ocean BGC</b>	1D slab	1D slab	n.a.	1D	n.a.	n.a.
<b>Area of model original tuning</b>	Arctic	Arctic	Arctic	Arctic	Antarctic	Arctic
<b>Reference</b>	Tedesco et al (2010)	Tedesco and Vichi (2014)	Duarte et al (2017)	Mortenson et al (2017)	Saenz and Arrigo (2014)	Castellani et al (2017)

138

139 The lead, approximately 400 m wide, opened on 23 April, began refreezing on 26 April, and was fully refrozen by 1 May.  
140 The newly formed young ice in the lead was sampled from 6 May along a 100 m-long transect extending from the edge of  
141 the lead toward its centre every 2–3 days until it broke up on 4 June (Kauko et al., 2017). The algal growth period occurred

142 in April and May. While the ice algal community was initially highly mixed, pennate diatoms of the genus *Nitzschia* became  
143 dominant later in the season.

144

145 The N-ICE2015 refrozen lead time series was chosen for this intercomparison based on two key factors:

146

147 • Observational data availability: It provides sufficient observations (Kauko et al., 2017) for comparison with model  
148 simulations of physico-biogeochemical variables.

149 • Ancillary data availability: It includes detailed time series of atmosphere and ocean data, necessary to force model  
150 runs, and has been tested for feasibility in a previous 1D modelling study (Duarte et al., 2017).

151

## 152 2.3 Experimental setup

153 A strict protocol was developed and followed by all modelling groups. To accommodate the diversity of models, a minimum  
154 set of variables was selected for comparison with observations. These included sea-ice season timing, ice thickness, and  
155 snow thickness for coupled physical-biogeochemical models, as well as sea-ice nutrient concentrations and algal biomass  
156 (represented by Chl-a) for all models.

157

158 Two distinct experiments were conducted to assess model performance. The first experiment, labelled *no tuning*, aimed to  
159 run each model in its default configuration. The primary objective was to analyze the differences between model outputs and  
160 observational data and quantify the extent of biases. The intercomparison within this experiment sought to identify potential  
161 reasons for deviations from observations, such as the omission of key processes or inadequate parameterisations. The second  
162 experiment, labelled *tuning*, involved adjusting the models to better align with observed physical and biogeochemical  
163 properties. This experiment aimed to identify which processes needed to be modified or added, as well as the specific  
164 parameterisations or parameters that were adjusted and fine-tuned to improve agreement with observations.

165

166 Both experiments were carried out independently by each modelling group, without prior knowledge of the work undertaken  
167 by others. This approach was adopted to eliminate potential biases, whether conscious or unconscious, during the  
168 implementation phase. To ensure a standardized comparison across models, all simulations used the same atmospheric and  
169 ocean forcing, as well as identical initial and boundary conditions, described in Duarte et al. (2017). Forcing time series  
170 included air temperature, precipitation, specific humidity, and wind speed (Hudson et al., 2015; Cohen et al., 2017); incident  
171 surface short and longwave radiation (Taskjelle et al., 2016; Hudson et al., 2016); sea ice temperature and salinity (Gerland  
172 et al., 2017); surface current velocity, heat fluxes, salinity, and temperature (Peterson et al., 2016, 2017); and ocean surface  
173 nutrient concentrations (Assmy et al., 2016). For the sea-ice biogeochemical model without a thermodynamic component  
174 (i.e., SIMBA), observed ice and snow thickness data were provided. This standardised approach improved the comparability

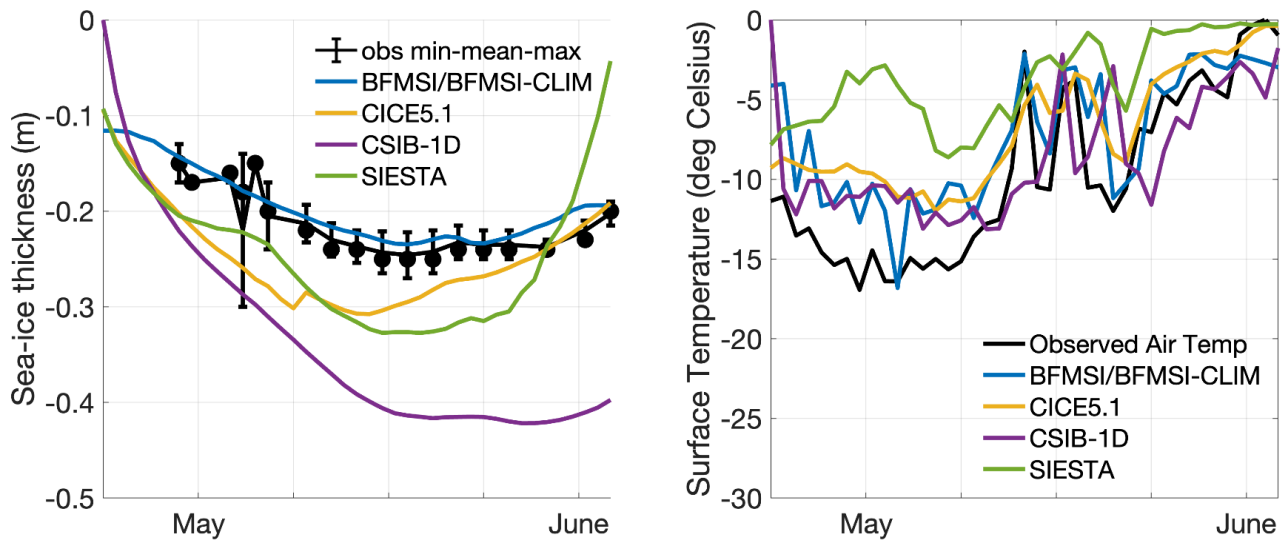
175 of the models, allowing for a robust evaluation of model performance. In the final phase, results were presented by each  
176 modelling group, and teams collaboratively discussed challenges, adjustments, and tuning choices.

### 177 3. Results and discussion

178 To support the interpretation of the biogeochemical models' performances, we first compared modelled and observed sea-ice  
179 physical properties, in particular sea-ice thickness and surface temperature (Fig. 1). We did not include snow thickness in this  
180 comparison, as observed values were relatively low and little variable, ranging between 2 and 6 cm between 7 May and 3  
181 June (Kauko et al., 2017) and thus had a limited influence on model differences for this specific case.

182

183 Observed sea-ice thickness shows relatively stable values around 0.2 m from early May to early June, with minor variability  
184 (Fig. 1). Models with thermodynamic components (BFMSI/BFMSI-CLIM, CICE5.1, CSIB-1D, and SIESTA) generally  
185 captured the observed thickness range and seasonal trend, although some diverge more notably. Surface temperature  
186 simulations show stronger deviations across models. Although all models follow the overall seasonal warming trend  
187 observed in the N-ICE2015 air temperature data (Fig. 1, right panel), the amplitude and short-term variability differ. While  
188 some models reproduce much of the daily variability, others exhibit smoother or warmer biases. These differences in  
189 physical conditions influenced light penetration and melt timing, which in turn affected the timing and magnitude of  
190 simulated algal blooms, which will be analysed next.



191

192 **Figure 1:** Model results for sea-ice thickness (left) and surface temperature (right). Observations of sea-ice thickness are shown as dots  
193 for the mean among replicates (at least 5 each) from different ice cores, while associated bars indicate the variability of the measurements  
194 between their maximum and minimum. The observed air temperature is part of the forcings provided to the modelling groups (Hudson et  
195 al., 2015; Cohen et al., 2017) and it is shown for comparison with modelled surface temperature.

196 Although the N-ICE refrozen lead resembles a typical ice season, in the *no tuning* experiment, none of the models accurately  
197 captured the observed algal phenology and bloom magnitude (Fig. 2, top left). All but one model underestimated Chl-a and  
198 produced a delayed bloom onset, though performances varied across diagnostic measures. Since most of the models tended  
199 to overestimate sea-ice thickness (Fig. 1), the delay in the simulated algal bloom could be attributed to reduced light  
200 transmittance through thicker ice. However, the delay also occurred in models that did not overestimate ice thickness,  
201 suggesting that other factors must have contributed to this bias. Due to limited nutrient data, few considerations can be drawn  
202 about simulated nutrient dynamics beyond an assessment of the potential model error's order of magnitude. Here, all but one  
203 model underestimated nitrate and silicate concentrations (Fig. 2, mid and bottom left), though all remained within a  
204 reasonable range.

205

206 In the *tuning* experiment, all models were able to reasonably simulate the ice algal phenology, though performance still  
207 varied across models (Fig. 2, top right). However, little improvement was achieved in the simulation of nitrate and silicate  
208 dynamics. Interestingly, tuning focused on different processes and parameters among models (Table 2), including:

209

- 210 • Change in the algal growth rate and/or in the size of the initial seeding population
- 211 • The possibility of downward vertical migration of algae during melting
- 212 • Magnitude of silicic acid limitation by changing the half saturation constant and/or the nitrogen: silicon ratio of ice  
213 algae and/or the reference quota of silicon in sea-ice algae.

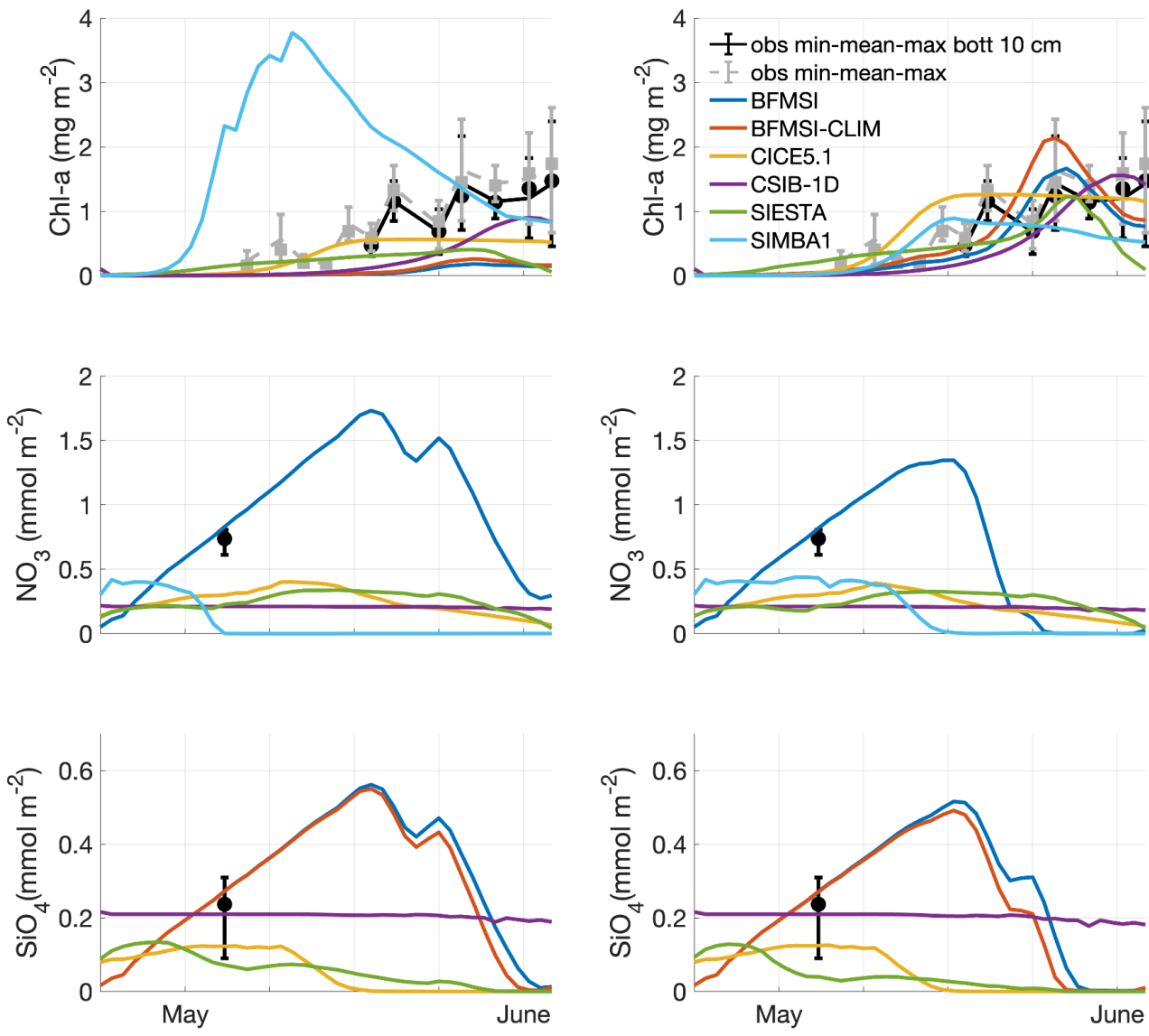
214

215 Overall, all tuning strategies aimed to either lessen nutrient limitation or increase algal seeding or growth. However, despite  
216 tuning efforts, none of the models significantly improved the simulation of nitrate magnitude, except for BFM-SI, which was  
217 also the only model that did not underestimate nitrate and silicate before tuning (Fig. 2, mid and bottom left). When  
218 comparing nutrient parameterisations across models (Table 1), BFM-SI stands out as the only model in which the variability  
219 of the dynamic sea-ice BAL modulates the upward fluxes of dissolved inorganic matter. CSIB-1D also performed well in  
220 simulating the silicate dynamics, matching the magnitude of the observations before and after tuning. For most models,  
221 silicon had the strongest effect on ice algal growth during tuning, suggesting a potentially dominant role of silicon limitation.  
222 This would also explain why SIMBA was the only model that did not underestimate, but rather overestimated, ice algal  
223 growth, since it did not include silicon among its limiting nutrients.

224

225 In general, models performed more poorly when simulating sea-ice nutrient dynamics. The limited improvement in nutrient  
226 representation compared to biomass can be attributed to model groups prioritising fitting simulations to Chl-a observations  
227 during the tuning phase, as these data were more temporally resolved and directly linked to the main focus of the study, i.e.,  
228 the ice algal bloom. In contrast, nutrient observations were limited to a single time point, which made them more difficult to

229 constrain reliably. Nevertheless, despite the scarcity of available data, the simulation of nutrient processes appears poorly  
 230 constrained, pointing to the need for more in-depth observational and experimental work.



231

232 **Figure 21:** Experiment with *no tuning* (left) and *tuning* (right). Model results for ice algae Chl-a (top), nitrate (middle), and silicate  
 233 (bottom). Observations are shown as dots for the mean of the entire ice core or the bottom 10 cm (5 replicates each), while associated bars  
 234 indicate the variability of the measurements between their maximum and minimum measures.

235 The *tuning* experiment highlights the diversity of tuning parameters across models (Table 2), prompting critical questions  
236 about model functionality and calibration. While models can be adjusted to align with observations, there is a risk of  
237 achieving accurate results for the wrong reasons, particularly when tuning compensates for a missing or misrepresented  
238 process. In our case, none of our models included young ice formation. Observations indicate that a consistent fraction of the  
239 sea-ice sampled from the refrozen lead was granular (Graham et al., 2019), formed as frazil ice in turbulent conditions. As  
240 turbulence subsides, frazil crystals rise and can entrain suspended particles, including biological material, during acent,  
241 effectively concentrating them in the newly forming ice (Weeks and Ackley, 1982, Janssen et al., 2018). This may explain  
242 some of the tuning strategies, such as increases in algal growth rate (CSIB-1D) or the size of the initial seeding population  
243 (BFM-SI, BFM-SI-Clim).

244

245 However, other factors likely influenced tuning choices as well. For example, some models used diatom Si:N ratios more  
246 appropriate for Antarctic waters, which overestimate the silica demand of Arctic diatoms. For example, CICE used a Si:N  
247 ratio close to 4:1, whereas Arctic diatoms may be closer to 1:1 (Duarte et al., 2017). In addition, the presence of relatively  
248 low Si:N ratios in Atlantic Water entering the region, as discussed in studies such as Duarte et al. (2021), supports the  
249 potential for silica limitation to emerge before nitrogen is exhausted. These regional nutrient characteristics and model  
250 structural features may have prompted tuning strategies involving relaxed silica limitation (BFM-SI, BFM-SI-Clim, CICE  
251 5.1, and SIESTA). Furthermore, the apparent need to reduce nutrient limitation in order to simulate realistic biomass may  
252 indicate that ocean-to-ice nutrient fluxes are underestimated in some models (Duarte et al., 2022).

253

254 Taken together, this intercomparison underscores how model tuning decisions can reveal not only numerical sensitivities but  
255 also areas where physical and biogeochemical process representations remain uncertain or incomplete. These insights are  
256 valuable for guiding future model development and targeted observations.

257

#### 258 4. Conclusions

259 This study presents an intercomparison of one-dimensional sea-ice biogeochemical models, evaluating their ability to  
260 simulate algal phenology, bloom magnitude, and nutrient dynamics in a refrozen lead environment. The results highlight  
261 significant disparities in model performance, with most models struggling to accurately reproduce the observed algal  
262 biomass and nutrient concentrations, for some models even after tuning. While adjustments improved the representation of  
263 ice algal phenology, they had a limited impact on nutrient concentration for most of the models, emphasizing the challenges  
264 of parameterizing key processes such as nutrient fluxes and reinforcing the need for continued model development and  
265 validation supported by dedicated field and experimental observations.

266

267

269 Table 2. Comparison among models' performances before and after tuning.

Model/ Properties	BFM-SI	BFM-SI-Clim	CICE 5.1	CSIB-1D	SIESTA	SIMBA
<b>Ice algal phenology before tuning</b>	Good algal growth timing but lower algal biomass.  Max [Chl-a]= 0.18 mg m <sup>-2</sup>  Day of the year of peak of Chl-a = 146	Good algal growth timing but lower algal biomass.  Max [Chl-a]= 0.26 mg m <sup>-2</sup>  Day of the year of peak of Chl-a = 146	Good algal growth timing but lower algal biomass.  Max [Chl-a]= 0.56 mg m <sup>-2</sup>  Day of the year of peak of Chl-a = 142	Good algal growth and lower algal biomass.  Max [Chl-a]= 0.90 mg m <sup>-2</sup>  Day of the year of peak of Chl-a = 152	Good algal growth timing but lower algal biomass.  Max [Chl-a] = 0.41 mg m <sup>-2</sup>  Day of the year of peak of Chl-a = 147	Earlier algal growth and higher algal biomass  Max [Chl-a]= 3.77 mg m <sup>-2</sup>  Day of the year of peak of Chl-a = 131
<b>Tuning strategy</b>	Lower silica limitation and higher algal biomass in seawater	Lower silica limitation and higher algal biomass in seawater	Lower silica limitation and reduced recruitment	Higher algal max spec growth rate	Active algal migration against brine movement and lower Si half-saturation constant.	Lower algal growth rate and removal of winter drainage of nutrients
<b>Parameter(s) before tuning</b>	Initial seawater [Chl-a] = 0.05 mg m <sup>-3</sup>  Rerefence Si quotum for adapted diatoms=0.0085 mmol m <sup>-3</sup>	Initial seawater [Chl-a] = 0.05 mg m <sup>-3</sup>  Rerefence Si quotum for adapted diatoms=0.0085 mmol m <sup>-3</sup>	Diatom Si:N ratio = 1.8 Half saturation for silicon uptake = 4.0 $\mu$ M Diatom boundary concentration = 0.002 $\mu$ M	Chl-a max spec growth rate = 0.85 d <sup>-1</sup>	Algae fixed in ice layer grid; Half saturation of silicon uptake = 4.0 $\mu$ M	Chl-a max spec growth rate = 0.86 d <sup>-1</sup>
<b>Parameter(s) after tuning</b>	Initial seawater [Chl-a] in = 0.5 mg m <sup>-3</sup>  Rerefence Si quotum for adapted diatoms=0.0025 mmol m <sup>-3</sup>	Initial seawater [Chl-a] in = 0.5 mg m <sup>-3</sup>  Rerefence Si quotum for adapted diatoms=0.0025 mmol m <sup>-3</sup>	Diatom Si:N ratio = 1.0 Half saturation for silicon uptake = 2.2 $\mu$ M Diatom boundary concentration = 0.0011 $\mu$ M	Chl-a max spec growth rate increased to 0.95 d <sup>-1</sup>	Algae allowed to migrate downward with ice growth, up to 1.5 cm d <sup>-1</sup> ; Half saturation of silicon uptake = 1.0 $\mu$ M	Chl-a max spec growth rate = 0.5 d <sup>-1</sup>
<b>Ice algal phenology after tuning</b>	Algal phenology and magnitude	Algal phenology and magnitude	Algal phenology and magnitude	Algal phenology and magnitude	Algal phenology	Algal phenology and magnitude

	within observed range; Nitrate and silicate within range.  Max [Chl-a] = 1.67 mg m <sup>-2</sup>  Day of the year of peak of Chl-a = 146	within observed range, Silicate within range.  Max [Chl-a] = 2.14 mg m <sup>-2</sup>  Day of the year of peak of Chl-a = 147	within observed range; Lower nitrate, Silicate within range.  Max [Chl-a] = 1.26 mg m <sup>-2</sup>  Day of the year of peak of Chl-a = 141	within observed range; Lower nitrate; Silicate within range.  Max [Chl-a] = 1.56 mg m <sup>-2</sup>  Day of the year of peak of Chl-a = 152	within observed range; Earlier algal decay; Lower silicate and nitrate.  Max [Chl-a] = 1.23 mg m <sup>-2</sup>  Day of the year of peak of Chl-a = 147	within observed range; Lower nitrate.  Max [Chl-a] = 0.89 mg m <sup>-2</sup>  Day of the year of peak of Chl-a = 137
--	--	--	---	---	--	--

270

271 The intercomparison highlights the unexpected challenges encountered in simulating a refrozen lead, primarily attributed to  
272 the short ice season and the difficulty most models faced in accumulating sufficient sympagic biomass. In a future Arctic  
273 Ocean characterized by increased lead openings, refreezing events, and young ice formation, there is an urgent need for  
274 models to be able to represent such a dynamic environment. This study underscores the importance of understanding and  
275 addressing the complexities involved in simulating specific and dynamic environmental scenarios.

276

277 The diversity of adjustments across models highlights both the range of tuning options available and the persisting  
278 knowledge gaps. The insights gained contribute valuable knowledge to ongoing efforts aimed at refining and improving  
279 numerical models, ensuring their accuracy and reliability in capturing complex interactions. To further advance this field of  
280 science, collaborative and harmonized modelling developments are recommended. Variability in tuning strategies  
281 underscores key knowledge gaps and the need for further model development using more coordinated approaches, such as  
282 common evaluation criteria and/or shared parameter ranges. In doing so, sea-ice biogeochemical modelling can build on  
283 lessons learned from open-ocean biogeochemical intercomparison and tuning efforts (e.g., Schartau et al., 2017), while  
284 addressing the unique challenges of simulating sympagic (i.e., in-ice) systems. A *Phase 2* of the intercomparison would be  
285 highly valuable, potentially extending the study to the variability of habitats that characterizes Antarctic sea ice.  
286 Collaborative sensitivity tests could be conducted, with all models evaluating biological responses to the same tuning  
287 adjustments, tuning options could be expanded, and standard parameter ranges could be revisited based on newer data  
288 collected in recent years. Increased clarity of model sensitivities would improve future model robustness and enhance  
289 confidence in simulations of biogeochemical processes in ice-covered oceans.

## 290 Code and data availability

291 All relevant data, model code and numerical simulations presented in this work will be publicly made available upon  
292 manuscript's acceptance.

### 293 Author contributions

294 LT and MV conceived the study. LT, GC, PD, EM, and BS produced the model runs. LT merged results from different  
295 models and wrote the first draft of the ms. All authors contributed to the analysis of results, discussion, and/or editing of the  
296 manuscript.

### 297 Competing interests

298 The authors declare no competing interests.

### 299 Acknowledgements

300 This work was written under the auspices of BEPSII (Biogeochemical Exchange Processes at the Sea-Ice Interfaces) Expert  
301 Group ([www.bepsii.org](http://www.bepsii.org)).

### 302 Financial support

303 LT and PD received funding from the European Union's Horizon 2020 research and innovation programme under grant  
304 agreement No 101003826 via project CRiceS (Climate relevant interactions and feedbacks: the key role of sea ice and snow  
305 in the polar and global climate system). GC, PD, and SM received funding from the RCN BREATHE project (Bottom sea ice  
306 Respiration and nutrient Exchanges Assessed for THE Arctic, #325405). PD and SM also received funding from the iC3  
307 Center of Excellence (Centre for ice, Cryosphere, Carbon and Climate, #332635). EM received funding through ArcticNet  
308 and the National Science and Engineering Council in Canada. NS acknowledges Fisheries and Oceans Canada. Two  
309 in-person workshops were organized by the BEPSII Expert Group (Biogeochemical Exchange Processes at Sea Ice  
310 Interfaces) to support this work. These workshops were financially supported by the Scientific Committee on Antarctic  
311 Research (SCAR) and the World Climate Research Programme (WCRP) Climate and Cryosphere (CliC) core project.

### 312 Supplementary Material

313

#### 314 S1 Model description

315

#### 316 **BFM-SI and BFM-SI-Clim**

##### 317 *Overview*

318 The Biogeochemical Flux Model for sea ice (BFM-SI, Tedesco et al., 2010) is derived from the Biogeochemical Flux Model

319 (BFM) framework (Vichi et al., 2023 and references therein), retaining its structure based on Chemical Functional Families  
320 (CFFs) and Living Functional Groups (LFGs). CFFs represent the elemental composition of living and non-living matter (C,  
321 N, P, Si, etc.), while LFGs describe groups of organisms with similar functional behavior.

322 The model simulates biogeochemical processes within the Biologically Active Layer (BAL, Tedesco et al., 2010), the  
323 time-varying, permeable fraction of sea ice where liquid brine channels remain interconnected and biological activity can  
324 occur. This dynamic layer, typically located at the ice bottom, evolves according to physical conditions (e.g., temperature,  
325 salinity, brine volume) computed by a sea-ice physical model. The biological model simulates algal growth and elemental  
326 cycling only within this layer, assuming all biomass is confined to the permeable ice fraction continuously connected to  
327 seawater, maintaining full mass conservation at the ice–ocean–atmosphere interfaces.

328 The sea-ice physical model used in this study is ESIM (Enhanced Sea Ice Model). ESIM is a sea-ice thermodynamic model  
329 originally based on the Semtner 0-layer model (Semtner, 1976), but with more physical processes. It was initially built as a  
330 1-D thermodynamic model of the sea-ice growth and decay (Tedesco et al., 2009), calculating vertical heat fluxes based on  
331 the 1-dimensional heat conduction equation. ESIM has been later enhanced with a halodynamic component (Tedesco et al.,  
332 2010). Initial salt entrapment, gravity drainage, and flushing processes have been added to simulate the salinity evolution of  
333 the sea ice. In addition, the model takes into account other processes such as different forms of snow metamorphism (snow  
334 compaction, snow ice and superimposed ice formation). ESIM has been developed targeting biological applications, thus  
335 with a focus on the physical requirements to model the biogeochemistry of the sea ice. The feature that makes this coupling  
336 possible is the innovative concept of the sea-ice BAL (Tedesco et al., 2010). The application of the BAL concept is more  
337 realistic than a prescribed static bottom BAL and is lighter than multi-layer models, thus it is suitable for large-scale  
338 applications without losing performance (Tedesco and Vichi, 2010, 2014).

### 339 *State variables and structure*

340 BFM-SI resolves 28 state variables organized as:

- 341     ● 2 LFGs for sea-ice algae:
  - 342         1. Adapted diatoms (20–200 µm; Si-limited, highly acclimated)
  - 343         2. Surviving nanoflagellates (2–20 µm; low acclimation capacity)
- 344     ● 1 LFG for sea-ice fauna
- 345     ● 1 LFG for sea-ice bacteria
- 346     ● 6 inorganic CFFs: phosphate, nitrate, ammonium, silicate, oxygen, carbon dioxide.
- 347     ● 2 organic non-living CFFs: dissolved and particulate detritus.

348 Each algal group is described by up to five state variables (C, N, P, Si, and Chl), while ice fauna and bacteria up to three state  
349 variables (C, N, P, ). The model includes four macronutrients (phosphate, nitrate, ammonium, silicate), oxygen, and two  
350 detrital pools (dissolved and particulate, featuring up to 4 state variables C, N, P, Si). Biological processes include primary  
351 production respiration, exudation, nutrient uptake, lysis, and chlorophyll synthesis, with flexible stoichiometry  
352 (C:N:P:Si:Chl).

353 BFM-SI-Clim (Tedesco et al., 2014) is a simplified version of BFM-SI, retaining the same ecological dynamics, but  
354 including a reduced number of state variables. BFM-SI-Clim features only one single limiting macronutrient (Si) and one  
355 single group of sea ice algae (i.e. ice diatoms), same detritus detritus and gases for totally 11 state variables.

### 356 *Coupling and boundary fluxes*

357 BFM-SI and BFM-SI-Clim are coupled online to the pelagic BFM with matching LFGs and CFFs.

358     • Ice-ocean fluxes: The entrainment or release of dissolved and particulate matter is proportional to ice growth/melt  
359       rate and brine volume.

360     • Ice-atmosphere fluxes: The nutrient input from snow and precipitation can be considered and scaled to snow-melt  
361       rate.

362 These exchanges ensure conservation of mass and consistent carbon, nutrient, and gas cycling across the interfaces.

### 363 *Applications and relevance*

364 BFM-SI represents the first process-based, biomass-explicit sea-ice biogeochemical model within a generalized marine  
365 biogeochemical framework. It can be used as a standalone 1-D module (Tedesco et al., 2010; Tedesco et al., 2012; Tedesco et  
366 al., 2014) or in coupled online or offline configuration to 3-D ocean circulation models (Tedesco et al., 2017; Tedesco et al.,  
367 2019) to study seasonal productivity, biomass export, and the contribution of sea-ice biogeochemistry to the global carbon  
368 cycle.

369

370 **CICE 5.1**

### 371 *Overview*

372 A comprehensive description of the Los Alamos Sea Ice Model physics and biogeochemistry may be found in Hunke et al.  
373 (2015) and Jeffery et al. (2016). The implementation used in the present work is detailed in Duarte et al. (2017). Therefore,  
374 in the next paragraphs we provide only a brief description of the model based on the cited references. There are two main  
375 approaches to simulate biogeochemical processes with CICE: one based on bottom ice biogeochemistry and another based  
376 on vertically-resolved biogeochemistry, which was used in the present study. This configuration uses a biogrid of variable

377 height which overlaps part of the physical grid, used to compute thermodynamic processes. The number of layers of both  
378 grids is the same but their vertical resolution differs. The vertical extent of the biogrid is defined by the brine height which  
379 represents the sea ice vertical extent with an active brine network.

380 *State variables and structure*

381 The number of biogeochemical state variables in CICE biogeochemistry depends on user-defined options. In the simulations  
382 presented herein, these included brine height, the concentrations of nitrate, ammonia, silicic acid and diatom nitrogen. Brine  
383 concentrations are used for internal calculations and bulk values stored in model output files. The brine is exchanged across  
384 the layers of the biogrid and across the ice-ocean interface. These exchanges include brine drainage, driven by hydrostatic  
385 instability, and diffusion, driven by concentration gradients. Other exchanges occur during freezing and melting. In the case  
386 of sea ice inundation or snow melt, exchanges occur also at the ice-snow or ice-atmosphere interface. The biogeochemical  
387 model uses nitrogen as its “currency”. The model computes nutrient and silicic acid (in the case of diatoms) uptake by ice  
388 algae, remineralization and nitrification. Ice algal growth and production may be light, temperature or nutrient limited  
389 (nitrogen and silica, in the case of diatoms), following the Liebig’s law of minimum. Some tracers may cling to the ice  
390 matrix, such as ice algae, resisting expulsion during desalination, unlike dissolved nutrients.

391 *Coupling and boundary fluxes*

392 The CICE model may be coupled with ocean models and atmospheric models. We used a standalone configuration with an  
393 ocean slab layer as the bottom boundary. Time series of current velocities, heat fluxes, salinity, temperature, and nutrient  
394 concentrations forced the model. The atmosphere boundary was implemented using time series of air temperature, humidity,  
395 short and long wave radiation, precipitation, and wind velocity.

396 *Applications and relevance*

397 The CICE model is a community-type model used in several Earth System Models. It is one of the few models resolving  
398 biogeochemistry vertically.

399

400 **CSIB-1D**

401 *Overview*

402 The Canadian Sea Ice Biogeochemistry 1-Dimensional (CSIB-1D) model simulates ice algae and changes to nutrients within  
403 the ice. It is designed to simulate a sympagic ecosystem and biogeochemical processes coupled to a pelagic ecosystem in the

404 underlying water column in order to represent the Arctic marine environment. An in-depth description of the development  
405 and application of this model can be found in Mortenson et al. (2017).

#### 406 *State variables and structure*

407 The CSIB-1D ecosystem is represented by one functional sea-ice algal group dependent on three nutrients (silicate, nitrate  
408 and ammonium) in the lower skeletal layer of the sea ice, set as a default in the bottom 3 centimeters of the ice. The sea ice  
409 algae are limited by nutrients, light, and ice melt. The model uses a subgrid-scale non-uniform snow depth distribution to  
410 represent gradual snow melt and formation of melt ponds impacting light transmissions and heat fluxes during melt periods  
411 (Abraham et al., 2015). CSIB-1D ice algae are meant to represent diatoms, prevalent in the Arctic sea ice environment.

412 The ocean biogeochemistry model is a ten-compartment (small and large phytoplankton, microzooplankton,  
413 mesozooplankton, small and large detritus, biogenic silica, nitrate, ammonium, and silicate) based on Steiner et al. (2006).  
414 The module was updated by including mesozooplankton as a prognostic.

#### 415 *Coupling and boundary fluxes*

416 Exchange of nutrients between the skeletal layer and the water column is by molecular diffusion and parameterized based on  
417 currents at the ice-water interface. The model is coupled to a physical-biogeochemical ocean model based on the General  
418 Ocean Turbulence Model (GOTM). GOTM provides the physical quantities required for computation of biogeochemical  
419 variables in the water column, such as horizontal velocity fields, turbulent transports, photosynthetically active radiation  
420 (PAR), and temperature. They contribute to pelagic diatoms and detritus following Lavoie et al. (2009): sloughed ice algae  
421 enter either the large phytoplankton pool in which they continue to grow or the large detritus pool in which they sink rapidly  
422 as aggregate products in the coupled ocean model.

#### 423 *Application and Relevance*

424 CSIB has been applied to studies on the evolution of the ice-water exchange of dissolved inorganic carbon (Mortenson et al.,  
425 2018) and ice-water-air exchange of dimethyl sulfide (Hayashida et al., 2017) in the marine Arctic.

426

#### 427 *SIESTA*

#### 428 *Overview*

429 The Sea-Ice Ecosystem State (SIESTA) model is a thermodynamic vertically-layered sea ice and snow model coupled to an  
430 algal ecosystem model. The model and associated equations and parameterizations are described in Saenz and Arrigo (2012,

431 2014). The model was developed to vertically resolve sea ice brine processes (and associated nutrient transfer), sea ice  
432 optics, shortwave radiation transfer, and the sea ice algal productivity that is controlled by those processes. The model uses a  
433 minimum layer thickness of 2 cm. When the snow or ice thicknesses become greater than is resolved by the maximum  
434 number of layers (snow: 26, ice: 42), model layers grow and shrink in an accordion-fashion to preserve 2 cm resolution at the  
435 surface and snow-ice boundaries.

#### 436 *State variables and structure*

437 Sea ice algae in SIESTA is represented by a single (diatom) class of algae with a fixed stoichiometry, with internal units of  
438 carbon (mg/m<sup>3</sup>). Algae may be present in any layer of sea ice. Besides algal carbon, the ecological state variables used by the  
439 SIESTA model include temperature, salinity, density, particulate organic carbon (detritus that is remineralized to liberate  
440 macronutrients), and 4 macronutrients (ammonium, nitrate, phosphate, silica). The model dynamically calculates sea ice  
441 brine density and volume, and has parameterizations of snow metamorphosis, sea ice surface melt and ponding, snow-ice  
442 formation, brine pumping and drainage, and enhanced convection in the skeletal layer of growing sea ice. Sea ice algae are  
443 considered motile and can migrate downward at a limited rate, but do not migrate upward and are considered released to the  
444 water column during bottom ice melt.

#### 445 *Coupling and boundary fluxes*

446 SIESTA simulations in this manuscript were forced by time series of surface atmospheric and surface ocean parameters.  
447 SIESTA is mass- and energy-conservative to the accuracy of its 1st-order implicit solver. Coupling at the surface boundary  
448 requires the following atmospheric parameters: air temperature, wind speed, air pressure, dew point temperature, cloud cover  
449 (or downward longwave radiation), downwelling shortwave radiation) total precipitation. Coupling at the lower boundary  
450 requires the following surface ocean parameters: temperature, salinity, and macronutrient concentrations (ammonia, nitrate,  
451 phosphate, silica). SIESTA calculates, and can return to coupled models, energy and mass fluxes from the snow/ice/brine.  
452 Boundary flux calculations in SIESTA are derived from CICE version 4 (Hunke and Lipscomb, 2008).

#### 453 *Applications and relevance*

454 SIESTA has been used to help bound the contribution of sea ice algae to overall Southern Ocean primary production (Saenz  
455 and Arrigo, 2014). SIESTA is also coupled to a 1-dimensional vertical ocean model (KPP-Ecosystem-Ice [KEI]) for  
456 investigation of dynamic-thermodynamic sea-ice-ocean-ecosystem controls and interactions (Saenz et al. 2023).

457

458 *SIMBA*

#### 459 *Overview*

460 A comprehensive description of the Sea Ice Model for Bottom Algae (SIMBA) can be found in Castellani et al. (2017).  
461 Different from Castellani et al. (2017) where the process of growth/melt was responsible for only algal loss, in the present  
462 study it is applied to nutrients as well, and it is responsible for nutrient replenishment in the bottom of the ice.

#### 463 *State variables and structure*

464 SIMBA resolves only 3 state variables:

465     ● 1 for sea-ice algae:  
466     ● 1 for nutrients (nitrate)  
467     ● 1 for detritus

468 The simulated biological processes are primary production and nutrient uptake, whereas respiration, mortality, and  
469 remineralization are taken as constant. Equations are solved in mmol N m-3. Equations are solved in the bottom of the ice,  
470 the thickness of the ice bottom can be set according to the available observations. In the case of N-ICE we use 10 cm.

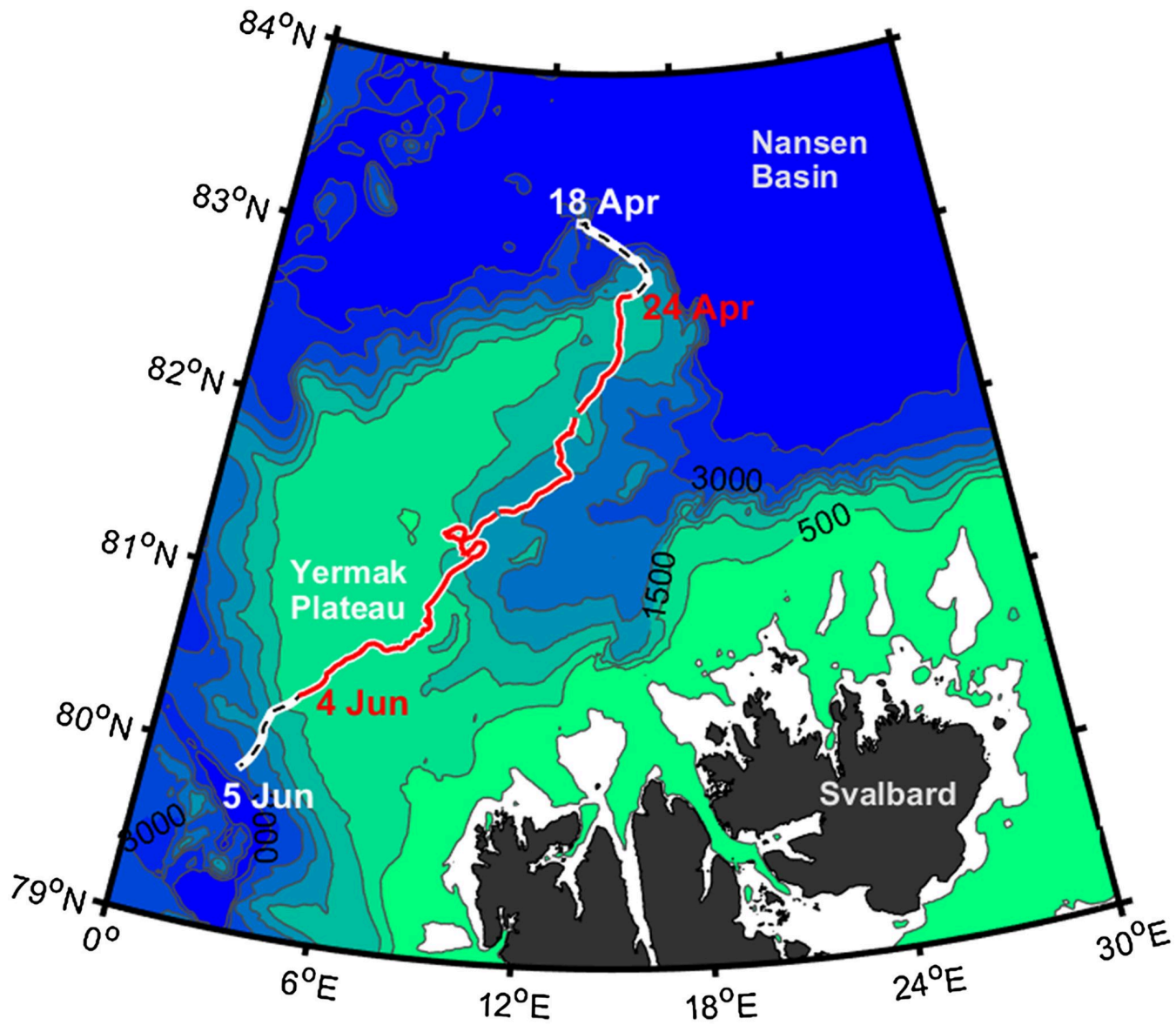
#### 471 *Coupling and boundary fluxes*

472 SIMBA is coupled with the underlying ocean through the growth and melt processes which are responsible for nutrient  
473 exchanges and for algal loss. Ocean variables (i.e., nutrients concentrations, ocean currents, and ocean temperature) must be  
474 provided as forcing. Other required forcing includes ice and snow thickness, integrated downward shortwave radiation, and  
475 atmospheric temperature.

#### 476 *Applications and relevance*

477 SIMBA was developed to study algal phenology on a pan-Arctic scale in two different environments: level ice and deformed  
478 ice. With this aim, SIMBA requires a prescribed physics. In Castellani et al. (2017) the physical constraints were provided by  
479 the MITgcm (Marshall et al., 1997; Losch et al, 2010). This characteristic of the model enhances its flexibility in applications  
480 and studies with different models (see e.g., Castellani et al., 2021).

481  
482



483

484 **Figure S1.** RV Lance drift between 18 April and 5 June 2015 during the drift of Floe 3 of the N-ICE2015 expedition, from  
485 the Nansen Basin and across the Yermak Plateau. The segment corresponding to the time span of the simulations described  
486 in this study is shown in red (Duarte et al., 2017).

487

488

489

490

491

## 492 References

493 Abraham, C., N. Steiner, A. Monahan, and C. Michel: Effects of subgrid-scale snow thickness variability on radiative  
494 transfer in sea ice, *J. Geophys. Res. Oceans*, 120, 5597–5614, doi:10.1002/2015JC010741, 2015.

495

496 Assmy, P., Duarte, P., Dujardin, J., Fernández-Méndez, M., Fransson, A., Hodgson, R., Kauko, H., Kristiansen, S., Mundy,  
497 C., Olsen, L. M., Peeken, I., Sandbu, M., Wallenschus, J., and Wold, A.: N-ICE2015 water column biogeochemistry  
498 [Dataset]. Norwegian Polar Institute, doi: 10.21334/NPOLAR.2016.3EBB7F64, 2016.

499

500 Arrigo, K.R.: Sea ice as a habitat for primary producers, In D.N. Thomas (Ed.), *Sea Ice* (3rd ed., pp. 352–369).  
501 Wiley-Blackwell, doi:10.1002/9781118778371.ch14, 2017.

502

503 Boetius, A., Albrecht, S., Bakker, K., Bienhold, C., Felden, J., Fernández-Méndez, M., Hendricks, S., Katlein, C., Lalande,  
504 C., Krumpen, T., Nicolaus, M., Peeken, I., Rabe, B., Rogacheva, A., Rybakova, E., Somavilla, R., and Wenzhöfer, F.: Export  
505 of algal biomass from the melting Arctic sea ice. *Science*, 339, 6126, 1430–1432, doi:10.1126/science.1231346, 2013.

506

507 Castellani, G., Losch, M., Lange, B. A., and Flores, H.: Modeling Arctic sea-ice algae: Physical drivers of spatial distribution  
508 and algae phenology, *J. Geophys. Res. Oceans*, 122, 7466–7487, doi:10.1002/2017JC012828, 2017.

509

510 Castellani, G., Tedesco, L., Steiner, N., Vancoppenolle, M.: Numerical model of sea-ice biogeochemistry, In D.N. Thomas  
511 (Ed.), *Sea Ice* (4th ed.). Wiley-Blackwell, In press doi:10.1002/9781394213764.ch20.

512

513 Castellani, G., Veyssiére, G., Karcher, M. et al. Shine a light: Under-ice light and its ecological implications in a changing  
514 Arctic Ocean, *Ambio* 51, 307–317, doi: 10.1007/s13280-021-01662-3, 2022.

515

516 Cohen, L., Hudson, S. R., Walden, V. P., Graham, R. M., and Granskog, M. A.: Meteorological conditions in a thinner Arctic  
517 sea ice regime from winter to summer during the Norwegian Young Sea Ice expedition (N-ICE2015), *J Geophys Res-Atmos*,  
518 122, 7235-7259, doi: 10.1002/2016JD026034, 2017.

519

520 Weeks, W. F., and Ackley, S. F. The growth, structure and properties of sea ice. CRREL Monogr. 82–1, 1982.

521

522 Dalman L. A., Meiners K. M., Thomas D. N., Deman F., Bestley S., Moreau S., Arrigo K. R., Campbell K., Corkill M.,  
523 Cozzi S., Delille B., Fransson A., Fraser A. D., Henley S. F., Janssens J., Lannuzel D., Munro D. R., Nomura D., Norman L.,

524 Papadimitriou S., Schallenberg C., Tison J.-L., Vancoppenolle M., van der Merwe P., Fripiat F.: Observation-based estimate  
525 of net community production in Antarctic sea ice. *Geophysical Research Letters*, 52, e2024GL113717, doi:  
526 10.1029/2024GL113717, 2025.

527

528 Duarte, P., Assmy, P., Campbell, K., and Sundfjord, A.: The importance of turbulent ocean–sea ice nutrient exchanges for  
529 simulation of ice algal biomass and production with CICE6.1 and Icepack 1.2, *Geosci. Model Dev.*, 15, 841–857, doi:  
530 10.5194/gmd-15-841-2022, 2022.

531 Duarte, P., Meyer, A., & Moreau, S.: Nutrients in water masses in the Atlantic sector of the Arctic Ocean: Temporal trends,  
532 mixing and links with primary production, *Journal of Geophysical Research: Oceans*, 126, e2021JC017413, doi:  
533 10.1029/2021JC017413, 2021.

534

535 Duarte, P., Meyer, A., Olsen, L. M., Kauko, H. M., Assmy, P., Rosel, A., Itkin, P., Hudson, S. R., Granskog, M. A., Gerland,  
536 S., Sundfjord, A., Steen, H., Hop, H., Cohen, L., Peterson, A. K., Jeffery, N., Elliott, S. M., Hunke, E. C., and Turner, A. K.:  
537 Sea ice thermohaline dynamics and biogeochemistry in the Arctic Ocean: Empirical and model results, *J. Geophys.  
538 Res.-Biogeo.*, 122, 1632–1654, doi: 10.1002/2016JG003660, 2017.

539

540 Eyring, V., Bony, S., Meehl, G. A., Senior, C. A., Stevens, B., Stouffer, R. J., and Taylor, K. E.: Overview of the Coupled  
541 Model Intercomparison Project Phase 6 (CMIP6) experimental design and organization, *Geosci. Model Dev.*, 9, 1937–1958,  
542 doi:10.5194/gmd-9-1937-2016, 2016.

543

544 Geoffroy, M., Bouchard, C., Flores, H., Robert, D., Gjøsæter, H., Hoover, C., Hop, H., Hussey, N. E., Nahrgang, J., Steiner,  
545 N., Bender, M., Berge, J., Castellani, G., Chernova, N., Copeman, L., David, C. L., Deary, A., Divoky, G., Dolgov, A. V.,  
546 Duffy-Anderson, J., Dupont, N., Durant, J. M., Elliott, K., Gauthier, S., Goldstein, E. D., Gradinger, R., Hedges, K., Herbig,  
547 J., Laurel, B., Loseto, L., Maes, S., Mark, F. C., Mosbech, A., Pedro, S., Pettitt-Wade, H., Prokopchuk, I., Renaud, P. E.,  
548 Schembri, S., Vestfals, C., Walkusz, W.; The circumpolar impacts of climate change and anthropogenic stressors on Arctic  
549 cod (*Boreogadus saida*) and its ecosystem. *Elementa: Science of the Anthropocene*, 11, 1: 00097. doi:  
550 10.1525/elementa.2022.00097, 2023.

551

552 Gerland, S., Granskog, M. A., King, J., and Rösel, A.: N-ICE2015 ICE core physics: Temperature, salinity and density [data  
553 set], Norwegian Polar Institute, doi: 10.21334/npolar.2017.c3db82e3, 2017.

554

555 Graham, R.M., Itkin, P., Meyer, A. et al.: Winter storms accelerate the demise of sea ice in the Atlantic sector of the Arctic  
556 Ocean. *Sci Rep* 9, 9222, doi: 10.1038/s41598-019-45574-5, 2019.

557

558 Granskog, M. A., Fer, I., Rinke, A., and Steen, H.: Atmosphere-Ice-Ocean-Ecosystem Processes in a Thinner Arctic Sea  
559 Ice Regime: The Norwegian Young Sea ICE (N-ICE2015) Expedition, *J. Geophys. Res.-Oceans*, 123, 1586–1594,  
560 doi: 10.1002/2017jc013328, 2018.

561

562 Hayashida, H., Jin, M., Steiner, N. S., Swart, N. C., Watanabe, E., Fiedler, R., Hogg, A. McC., Kiss, A. E., Matear, R. J., and  
563 Strutton, P. G.: Ice Algae Model Intercomparison Project phase 2 (IAMIP2), *Geosci. Model Dev.*, 14, 6847–6861,  
564 <https://doi.org/10.5194/gmd-14-6847-2021>, 2021.

565

566 Hayashida, H., Steiner, N., Monahan, A., Galindo, V., Lizotte, M., and Levasseur, M.: Implications of sea-ice  
567 biogeochemistry for oceanic production and emissions of dimethyl sulfide in the Arctic, *Biogeosciences*, 14, 3129–3155,  
568 doi: 10.5194/bg-14-3129-2017, 2017.

569

570 Hudson, S. R., Cohen, L., and Walden, V. P.: N-ICE2015 surface meteorology [data set], Norwegian Polar Institute,  
571 <https://doi.org/10.21334/npolar.2015.056a61d1>, 2015.

572

573 Hudson, S. R., Cohen, L., and Walden, V. P.: N-ICE2015 surface broadband radiation data [data set]. Norwegian Polar  
574 Institute, <https://doi.org/10.21334/npolar.2016.a89cb766>, 2016.

575

576 Hunke, E. C., and W. H. Lipscomb: CICE: The Los Alamos Sea Ice Model: Documentation and software user's manual,  
577 version 4.0, Tech. Rep. LA-CC-06-012, Los Alamos Natl. Lab., Los Alamos, N. M., 2008.

578

579 Hunke, E. C., Lipscomb, W. H., Turner, A. K., Jeffery, N., and Elliot, S.: CICE: The Los Alamos sea ice model  
580 documentation and user's manual version 5.1. Tech. Rep., LA-CC-06-012, Los Alamos National Laboratory, Los Alamos, N.  
581 M., 2015.

582

583 Janssens, J., Meiners, K. M., Townsend, A. T., Lannuzel, D.: Organic matter controls of iron incorporation in growing sea  
584 ice, *Frontiers in Earth Science* 6: 22, doi: 10.3389/feart.2018.00022, 2018.

585

586 Jeffery, N., Elliott, S., Hunke, E. C. , Lipscomb, W. H. and Turner, A. K.: Biogeochemistry of CICE: The Los Alamos Sea  
587 Ice Model, Documentation and User's Manual. Zbgc\_colpkg modifications to Version 5, Los Alamos National Laboratory,  
588 Los Alamos, N. M., 2016.

589

590 Kauko, H. M., Taskjelle, T., Assmy, P., Pavlov, A. K., Mundy, C. J., Duarte, P., Fernández-Méndez, M., Olsen, L. M.,  
591 Hudson, S. R., Johnsen, G., Elliot, A., Wang, F., Granskog, M. A.: Windows in Arctic sea ice: light transmission and ice  
592 algae in a refrozen lead, *J. Geophys. Res.-Biogeo.*, 122, doi:10.1002/2016JG003626, 2017.

593

594 Koch, C. W., Brown, T. A., Amiraux, R. et al. Year-round utilization of sea ice-associated carbon in Arctic ecosystems, *Nat  
595 Commun* 14, 1964, doi:10.1038/s41467-023-37612-8, 2023.

596

597 Kohlbach D., Lange B. A., Schaafsma, F. L., David, C., Vortkamp, M., Graeve, M., van Franeker, J. A., Krumpen, T., and  
598 Flores, H.: Ice Algae-Produced Carbon Is Critical for Overwintering of Antarctic Krill *Euphausia superba*, *Front. Mar. Sci.*  
599 4:310, doi:10.3389/fmars.2017.00310, 2017.

600

601 Lannuzel, D., Tedesco, L., van Leeuwe, M., Campbell, K., Flores, H., Delille, B., Miller, L., Stefels, J., Assmy, P., Bowman,  
602 J., Brown, K., Castellani, G., Chierici, M., Crabeck, O., Damm, E., Else, B., Fransson, A., Fripiat, F., Geilfus, N.-X.,  
603 Jacques, C., Jones, E., Kaartokallio, K., Kotovitch, M., Meiners, K., Moreau, S., Nomura, D., Peek, I., Rintala, J.-M.,  
604 Steiner, N., Tison, J.-L., Vancoppenolle, M., der Linden, F. V., Vichi, M., Wongpan, P.: The future of Arctic sea-ice  
605 biogeochemistry and ice-associated ecosystems, *Nature Climate Change*, doi:10.138/s41558-020-00940-4, 2020.

606

607 Losch, M., D. Menemenlis, J. M. Campin, P. Heimbach, and C. Hill: On the formulation of sea-ice models: Part 1: Effects of  
608 different solver implementations and parameterizations, *Ocean Modell.*, 33, 129–144, doi:10.1016/j.ocemod.2009.12.008,  
609 2010.

610

611 Marshall, J., A. J. Adcroft, C. N. Hill, L. Perelman, and C. Heisey: A finite-volume, incompressible Navier Stokes model for  
612 studies of the ocean on parallel computers, *J. Geophys. Res.*, 102(C3), 5753–5766, doi:10.1029/96JC02775, 1997.

613

614 Mortenson, E., Hayashida, H., Steiner, N., Monahan, A., Blais, M., Gale, M. A., Galindo, V., Gosselin, M., Hu, X., Lavoie,  
615 D., Mundy, C. J.: A model-based analysis of physical and biological controls on ice algal and pelagic primary production in  
616 Resolute Passage, *Elementa: Science of the Anthropocene Sci Anth*, 5, 39, doi:10.1525/elementa.229, 2017.

617

618 Mortenson, E., Steiner, N., Monahan, A. H., Miller, L. A., Geilfus, N.-X., & Brown, K., A model-based analysis of physical  
619 and biogeochemical controls on carbon exchange in the upper water column, sea ice, and atmosphere in a seasonally  
620 ice-covered Arctic strait. *Journal of Geophysical Research: Oceans*, 123, 7529–7549, doi: 10.1029/2018JC014376, 2018.

621

622 Olsen, L. M., Laney, S. R., Duarte, P., Kauko, H. M., Fernández-Méndez, M., Mundy, C. J., Rösel, A., Meyer, A., Itkin, P.,  
623 Cohen, L., Peek, I., Tatarek, A., Rózańska, M., Wiktor, J., Taskjelle, T., Pavlov, A. K., Hudson, S. R., Granskog, M. A.,

624 Hop, H., and Assmy, P.: The seeding of ice-algal blooms in Arctic pack ice: the multiyear ice seed repository hypothesis,  
625 Journal of Geophysical Research: Biogeosciences, 10.1002/2016jg003668, 2017.

626

627 Peterson, A. K., Fer, I., Randelhoff, A., Meyer, A., Håvik, L., Smedsrød, L. H., Onarheim, L., Muilwijk, M., Sundfjord, A.,  
628 and McPhee, M. H.: N-ICE2015 ocean turbulent fluxes from under-ICE turbulence cluster (TIC) [data set], Norwegian Polar  
629 Institute, <https://doi.org/10.21334/npolar.2016.ab29f1e2>, 2016.

630

631 Peterson, A. K., Fer, I., McPhee, M. G., and Randelhoff, A.: Turbulent heat and momentum fluxes in the upper ocean under  
632 Arctic sea ice, Journal of Geophysical Research: Oceans, 122, 1439–1456, doi:10.1002/2016JC012283, 2017.

633

634 Post, E., Bhatt, U. S., Bitz, C. M., Brodie, J. F., Fulton, T. L., Hebblewhite, M., Kerby, J., Kutz, S. J., Stirling, I., Walker D.  
635 A. et al.: Ecological consequences of sea-ice decline, Science, 341(6145), 519–524, doi:10.1126/science.1235225, 2013.

636

637 Poulin, M., Daugbjerg, N., Gradinger, R., Ilyash, L. V., Ratkova, T. N., von Quillfeldt, C.: The pan-Arctic biodiversity of  
638 marine pelagic and sea-ice unicellular eukaryotes: a first-attempt assessment, Mar. Biodiv., 41, 13–28,  
639 doi:10.1007/s12526-010-0058-8, 2011.

640

641 Saenz, B. T., and Arrigo, K. R.: Simulation of a sea ice ecosystem using a hybrid model for slush layer desalination, J.  
642 Geophys. Res., 117, C05007, doi:10.1029/2011JC007544, 2012.

643

644 Saenz, B. T., and Arrigo, K. R.: Annual primary production in Antarctic sea ice during 2005–2006 from a sea ice state  
645 estimate, J. Geophys. Res. Oceans, 119, 3645–3678, doi:10.1002/2013JC009677, 2014.

646

647 Saenz, B. T., McKee, D. C., Doney, S. C., Martinson, D. G., Stammerjohn, S. E: Influence of seasonally varying sea-ice  
648 concentration and subsurface ocean heat on sea-ice thickness and sea-ice seasonality for a ‘warm-shelf’ region in Antarctica.  
649 Journal of Glaciology, 69(277):1466-1482, doi:10.1017/jog.2023.36, 2023.

650

651 Schaafsma, F. L., D. Kohlbach, C. David, B. A. Lange, M. Graeve, H. Flores, and J. A. van Franeker: Spatio-temporal  
652 variability in the winter diet of larval and juvenile Antarctic krill, *Euphausia superba*, in ice-covered waters, Marine Ecology  
653 Progress Series, 580, 101-115, doi: [doi.org/10.3354/meps12309](https://doi.org/10.3354/meps12309), 2017.

654

655 Semtner, A. J.: A model for the thermodynamic growth of sea ice in numerical investigation of climate, J. Phys. Oceanogr.,  
656 6:379–389, doi: 10.1175/1520-0485(1976)006<0379:AMFTTG>2.0.CO;2, 1976.

657

658 Schartau, M., Wallhead, P., Hemmings, J., Löptien, U., Kriest, I., Krishna, S., Ward, B. A., Slawig, T., and Oschlies, A.:  
659 Reviews and syntheses: parameter identification in marine planktonic ecosystem modelling, *Biogeosciences*, 14, 1647–1701,  
660 doi: 10.5194/bg-14-1647-2017, 2017.

661

662 Steiner, N., Bowman, J., Campbell, K., Chierici, ...M., Eronen-Rasimus, Falardeau , E. M., Flores, H., Fransson , A., Herr ,  
663 H., Insley , S. J., Kauko, H., Lannuzel, D., Loseto, L., Lynnes , A., Majewski , A., Meiners , K., Miller, L.. A., Michel, L.,  
664 Moreau, S., Nacke , M., Nomura, D., Tedesco, L., van Franeker, J. A., van Leeuwe, M. A., Wongpan, P.: Climate change  
665 impacts on sea-ice ecosystems and associated ecosystem services, *Elem Sci Anth*, 9 (1): 00007,  
666 doi:10.1525/elementa.2021.00007, 2021.

667

668 Taskjelle, T., Hudson, S. R. , Pavlov, A., and Granskog, M. A.: N-ICE2015 surface and under-ICE spectral shortwave  
669 radiation data [data set], Norwegian Polar Institute, <https://doi.org/10.21334/npolar.2016.9089792e>, 2016.

670

671 Tedesco, L., Vichi, M., Haapala, J., Stipa, T.: An enhanced sea-ice thermodynamic model applied to  
672 the Baltic Sea. *Boreal Environmental Research* 14, 68–80.<http://www.borenv.net/BER/pdfs/ber14/ber14-068.pdf>, 2009.

673

674 Tedesco, L., Miettunen E., An, B.W., Kaartokallio, H., Haapala, J.: Long-term mesoscale variability of modelled sea-ice  
675 primary production in the northern Baltic Sea. *Elem. Sci. Anth.*, 5: 29, doi: 10.1525/elementa.223, 2017.

676

677 Tedesco, L., Vichi, M.: Sea ice biogeochemistry: a guide for modellers, *PLOS ONE*, doi:10.1371/journal.pone.0089217,  
678 2014.

679

680 Tedesco, L., Vichi, M., Haapala, J., and Stipa, T.: A dynamic Biologically-Active Layer for numerical studies of the sea ice  
681 ecosystem, *Ocean Modelling*, 35(1-2):89-104, doi:10.1016/j.ocemod.2010.06.008, 2010.

682

683 Tedesco, L., Vichi, M., Scoccimarro, E.: Sea-ice algal phenology in a warmer Arctic, *Science Advances*,5, eaav4830, doi:  
684 10.1126/sciadv.aav4830, 2019.

685

686 Tedesco, L., Vichi, M., Thomas, D.: Process studies on the ecological coupling between sea ice algae and phytoplankton,  
687 *Ecological Modelling*, 226: 120-138, doi:10.1016/j.ecolmodel.2011.11.011, 2012.

688

689 Watanabe, E., Jin, M., Hayashida, H., Zhang, J., & Steiner, N.: Multi-Model Intercomparison of the Pan-Arctic Ice-Algal  
690 Productivity on Seasonal, Interannual, and Decadal Timescales, *Journal of Geophysical Research: Oceans*, 124, 9053–9084.  
691 doi:10.1029/2019JC015100, 2019.